Miller, T.W., *et al*.- Supplementary Data

Figure S1- Connectivity Mapping reveals increased PI3K/mTOR signaling in LTED cells. Cells were treated with 10% DCC-FBS for 24 hrs, and RNA was harvested and analyzed using gene expression microarrays. Each LTED cell line profile was compared to its respective parental control profile, and probe sets with expression altered ≥1.3-fold (FDR-adjusted $p \leq 0.05$) were identified. The probe sets altered in each LTED/parental comparison were compared using a Venn Diagram to identify those commonly dysregulated in all four LTED lines. Such common probe sets were filtered for compatibility with the HG-U133A Affymetrix platform, which was used to generate the Connectivity Map (19). The resulting 45 probe sets (covering 35 genes, below) were used to query the Connectivity Map. We found significant discordance (negative enrichment) with gene signatures induced by the mTOR inhibitor sirolimus (rapamycin) and the PI3K inhibitor wortmannin.

Probe Sets downregulated in 4 LTED lines	
Probe Set ID	Gene Symbol
209460_at	ABAT
215465_at	ABCA12
201034_at	ADD3
201752_s_at	ADD3
205882_x_at	ADD3
203685_at	BCL2
207655_s_at	BLNK
212551_at	CAP2
212554_at	CAP2
206754_s_at	CYP2B6 /// CYP2B7P1
207147_at	DLX2
218976_at	DNAJC12
203303_at	DYNLT3
205031_at	EFNB3
205862_at	GREB1
203913_s_at	HPGD
203914_x_at	HPGD
211548_s_at	HPGD
203424_s_at	IGFBP5
211958_at	IGFBP5
211959_at	IGFBP5
204686_at	IRS1
209185_s_at	IRS2
209205_s_at	LMO4
222307_at	LOC282997
221760_at	MAN1A1
205413_at	MPPED2
205555_s_at	MSX2
210319_x_at	MSX2
212509_s_at	MXRA7
204105_s_at	NRCAM
217226_s_at	SFXN3
213624_at	SMPDL3A
203373_at	SOCS2
209813_x_at	TARP
211144_x_at	TARP /// TRGC2
215806_x_at	TARP /// TRGC2
216920_s_at	TARP /// TRGC2
209747_at	TGFB3
201666_at	TIMP1
219768_at	VTCN1

Probe Sets upregulated in 4 LTED lines	
Probe Set ID	Gene Symbol
219555_s_at	CENPN
202345_s_at	FABP5
219157_at	KLHL2
205632_s_at	PIP5K1B

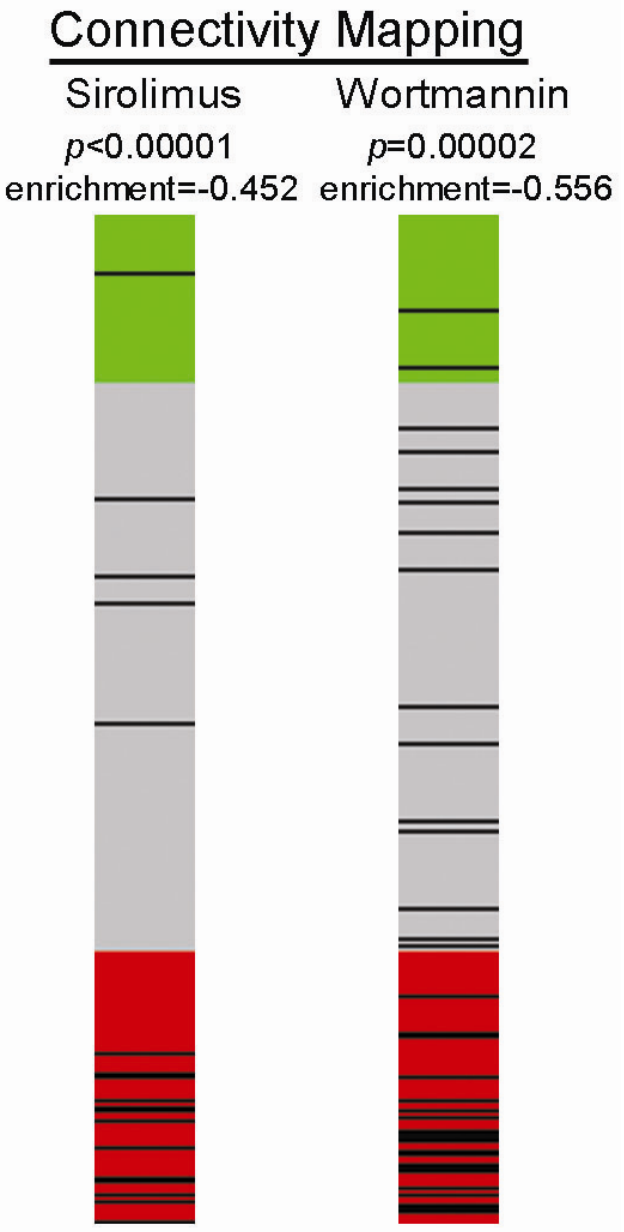

Figure S2- Pathway analysis of gene expression profiles reveals altered ‘IGF pathway’ genes in LTED cells. Sets of genes with expression altered ≥1.5-fold ($p \leq 0.05$) by microarray analysis within each LTED/parental cell line comparison were evaluated using Ingenuity Pathways Analysis software, which groups gene products by biological function. *Top*: Schematic of proteins involved in ‘IGF signaling’. *Bottom*: Genes encoding proteins involved in ‘IGF signaling’ which were significantly altered in LTED cells.

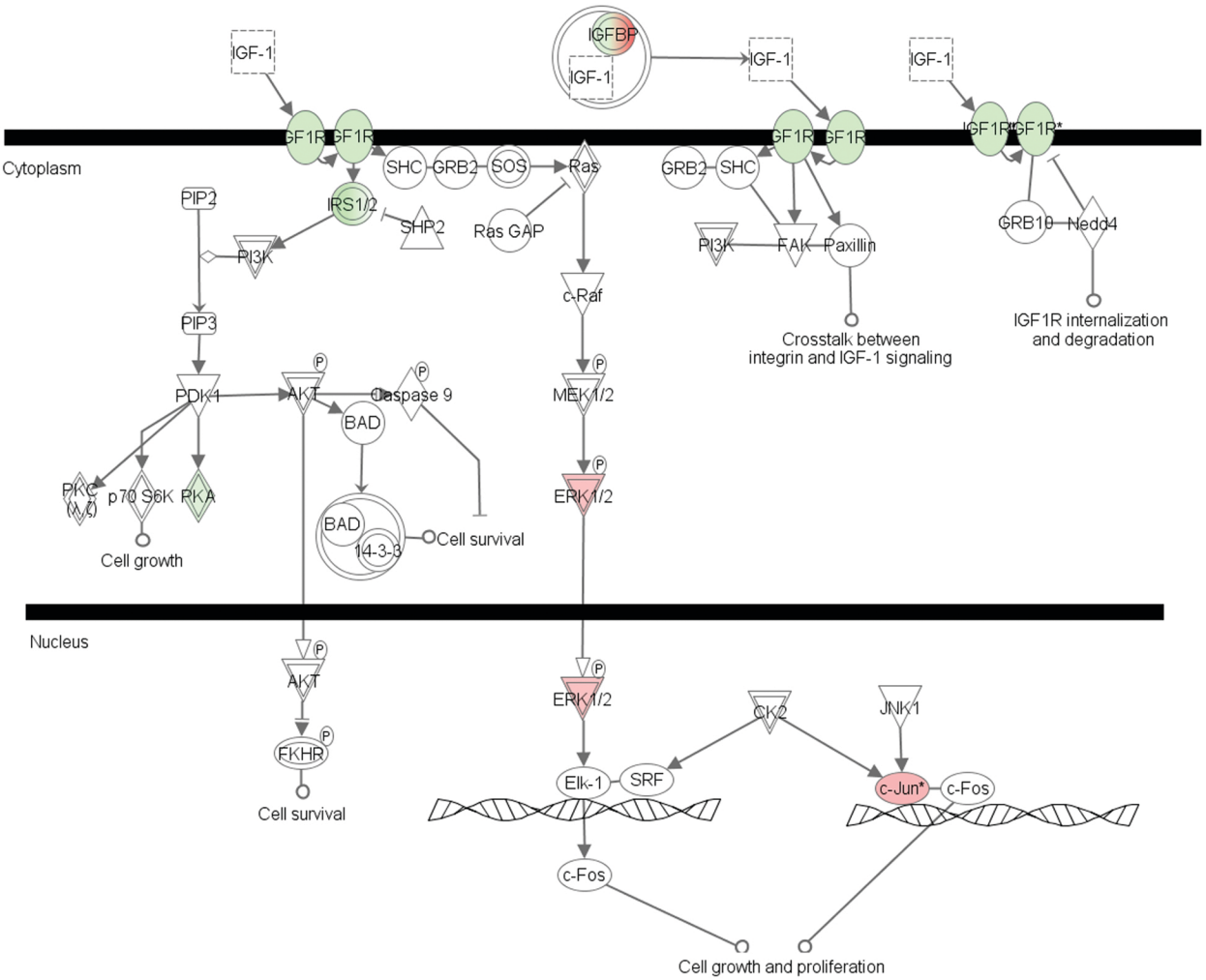

MCF-7	
IGF pathway *p* = .0049	
Gene	Fold-change (LTED/parental)
IGF1R	-3.45
IGFBP3	1.87
IGFBP5	-2.55
IGFBP5	-1.55
IGFBP6	-1.78
IRS1	-4.52
IRS1	-3.03
IRS2	-1.63
IRS2	-1.56
JUN	2.04
MAPK1	1.72
NOV	4.59
PRKAR2B	-1.65

MDA-361	
IGF pathway *p* = .00089	
Gene	Fold-change (LTED/parental)
GRB10	-2.02
IGF1R	-2.34
IGFBP4	-3.03
IGFBP5	-6.81
IGFBP5	-69.83
IRS1	-2.41
RASA1	-2.01

ZR75-1	
IGF pathway *p* = .357	
Gene	Fold-change (LTED/parental)
AKT3	-6.61
GRB10	-2.10
IGFBP2	-1.68
IGFBP4	-3.60
IGFBP5	-9.10
IGFBP5	-100.00
IRS1	-2.52
IRS2	-3.57
IRS2	-5.06
PIK3CA	-1.59
PXN	-1.51

HCC-1428	
IGF pathway *p* = .0087	
Gene	Fold-change (LTED/parental)
CTGF	-1.84
GRB10	-1.85
IGFBP4	-1.61
IGFBP5	2.11
IGFBP5	1.62
IGFBP7	-7.64
IRS1	-2.89
IRS1	-2.69
NEDD4	-1.63
PIK3R1	-1.63
PRKAR2B	-2.33
PRKCH	1.65

Figure S3- LTED cells are dependent upon receptors for IGF-IR and insulin for growth, and IGF-IR/InsR activation in primary breast tumors predicts poor outcome following endocrine therapy in patients. A-B) Cells were transiently transfected with siRNA targeting *IGF-IR*, *InsR*, or non-silencing control (siCon). Cells were then reseeded for growth assay (A) or immunoblotting (B). In growth assays, cells were treated with 10% DCC-FBS for 6 days (medium was replenished after 3 days), trypsinized and counted. Data are presented as % parental siCon (MCF-7 and ZR75-1 lines) or % siCon (HCC-1428/LTED), mean of triplicates ± SD. Data were analyzed using two-way ANOVA (MCF-7 and ZR75-1 lines) or one-way ANOVA (HCC-1428/LTED). *p<0.001 by Bonferroni post-hoc test corrected for multiple comparisons compared to siCon for each cell line. In immunoblotting assays, cells were treated with 10% DCC-FBS for three days. At this time, protein lysates were prepared and analyzed by immunoblotting using the indicated antibodies. C) Lysates from 64 hormone receptor-positive human breast tumors were analyzed by RPPA using antibodies against P-IGF-IR$\beta_{Y1135/1136}$ and IGF-IRβ. Patients were dichotomized based on mean cutoff of phospho/total IGF-IRβ ratio, and Kaplan-Meier recurrence curves of the upper and lower halves of patients were compared by log-rank test. The number of patients at risk of recurrence at different time points is noted below.

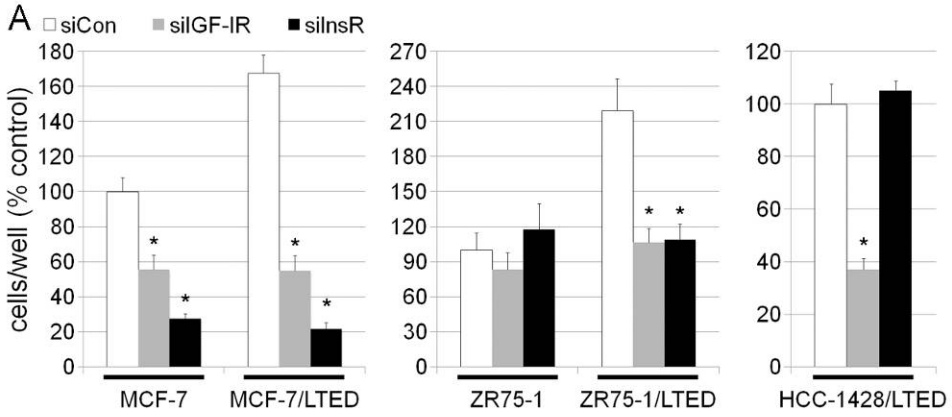

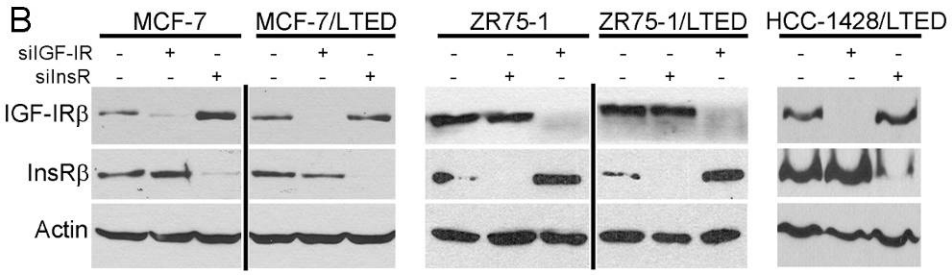

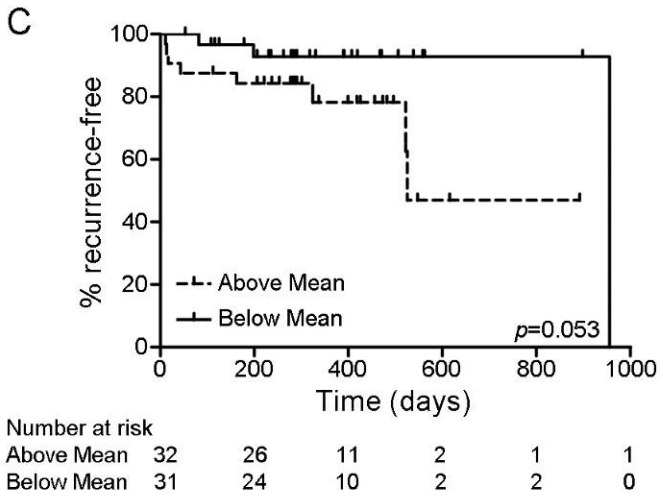

Figure S4- Inhibition of RTK phosphorylation with the small molecules AEW541 and lapatinib. A) MCF-7 cells were pretreated overnight with AEW541 in serum-free medium to block IGF-IR/InsR kinase signaling, then stimulated ± IGF-I or insulin ± AEW541 for 5 min. prior to lysis. IGF-I binds predominantly IGF-IR homodimers and IGF-IR/InsR heterodimers, while insulin binds InsR homodimers. Since AEW541 treatment blocked both IGF-I- and insulin-induced signaling, we infer that AEW541 inhibits both IGF-IR and InsR tyrosine kinases. B) MDA-361 cells were treated for 5 hours ± lapatinib prior to lysis. Lysates were analyzed by immunoblotting with the indicated antibodies.

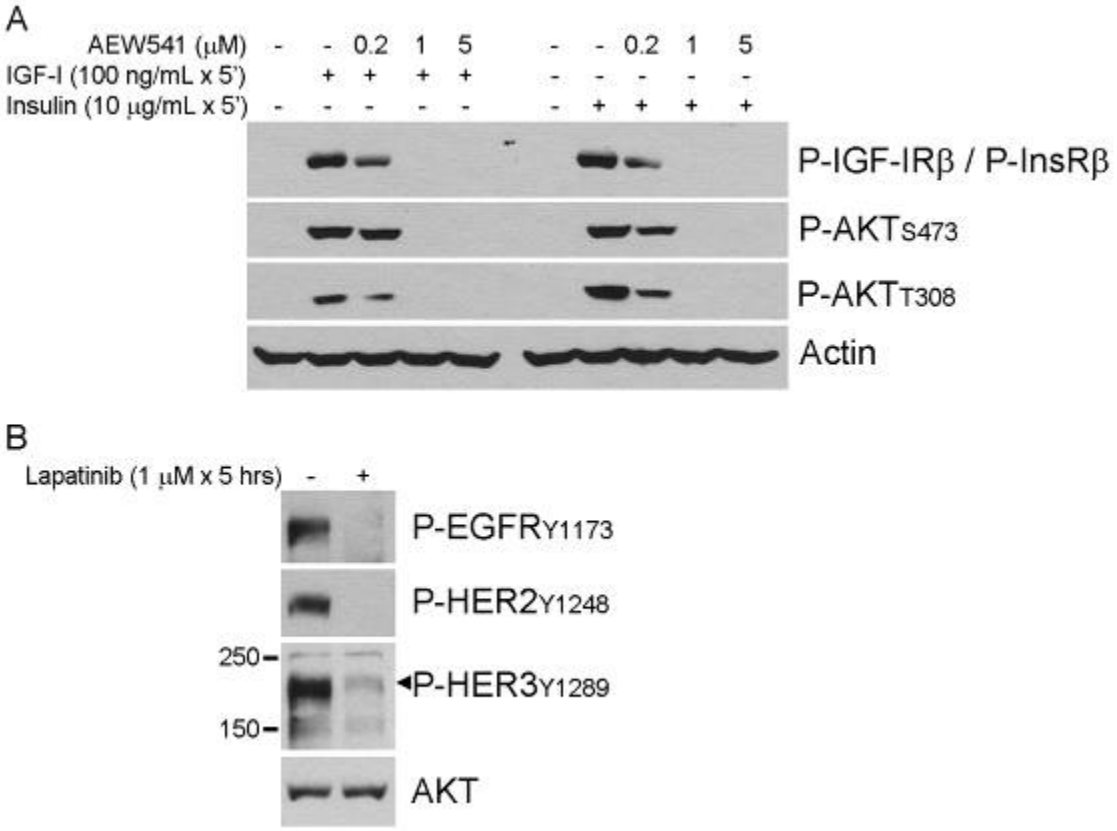

Figure S5- PI3K inhibition blocks anchorage-independent, hormone-independent colony formation. Cells were embedded in 0.4% soft agar with 5% DCC-FBS, and treated ± 200 nM BEZ235, 20 nM RAD001, 1 μM AEW541, 1 μM lapatinib, or the combination of AEW541 + lapatinib for 8-17 days. Wells were scanned using GelCount software, and colonies measuring 25-250 μm in diameter were counted. Wells were visually inspected to confirm drug effects (not shown). Data are presented as mean of triplicates ± SD. Data are presented as mean of triplicates ± SD. Data were analyzed using two-way ANOVA. *p<0.05, **p<0.01 by Bonferroni post-hoc test corrected for multiple comparisons compared to control within each cell line, unless otherwise indicated with brackets.

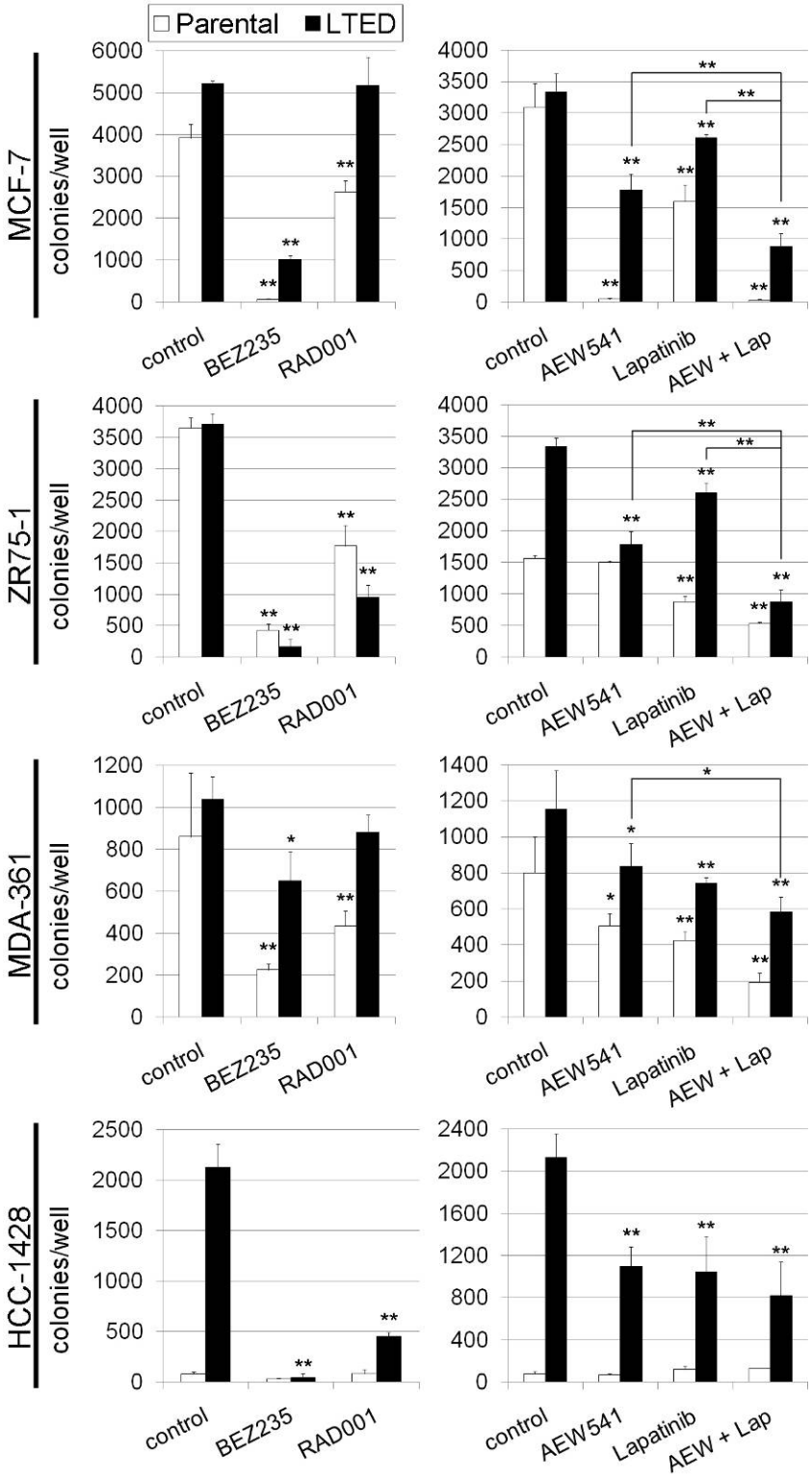

Figure S6- PI3K pathway inhibition induces apoptosis and prevents the emergence of hormone-independent cells. A) Parental cells were treated with 10% DCC-FBS ± the indicated kinase inhibitors. Media and drugs were replenished every 2-3 days. When control wells reached 40-60% confluence, cells were fixed and stained with crystal violet. Representative images are shown. *Inset*: microscopic field at 40x magnification. Quantification of staining intensity is shown at right as mean of triplicates ± SD (% control). Data were analyzed using one-way ANOVA. *p<0.01 by Bonferroni post-hoc test corrected for multiple comparisons compared to control. B) Cells were treated with 1% DCC-FBS ± 200 nM BEZ235 or 20 nM RAD001 for 3 days before fixation. Apoptotic cells were stained using an FITC-BrdU terminal deoxynucleotidyl labeling kit plus propidium iodide, followed by flow cytometry analysis (10,000 events counted). Percent of gated cells which showed FITC-BrdU labeling and/or sub-G1 levels of DNA were considered apoptotic. Data are presented as mean of triplicates ± SD. Data were analyzed using two-way ANOVA. *p<0.001 by Bonferroni post-hoc test corrected for multiple comparisons compared to control within each cell line.

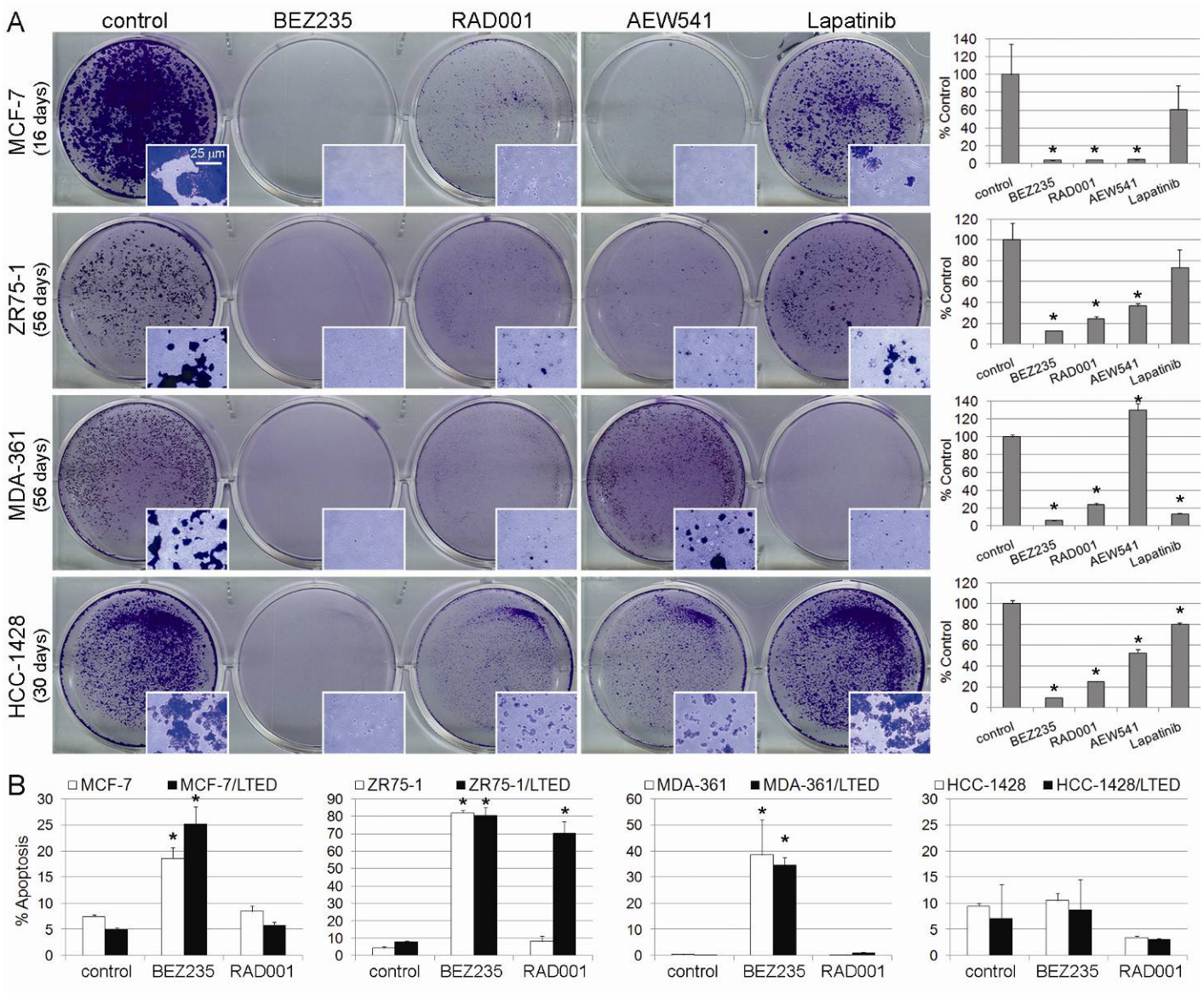

Miller, T.W., *et al*. Supplementary Methods

Antibody microarray analysis. Cells were treated for 24 hours with 1% DCC-FBS. Protein lysates were quantitated using BCA assay (Pierce). Lysates from parental cells were labeled with one fluorescent dye, and lysates from LTED cells were labeled with another fluorescent dye (performed by Kinexus Bioinformatics). Paired LTED and parental samples were mixed at a 1:1 ratio, and mixtures were used to probe microarrays containing immobilized antibodies against 652 antigens in duplicate (performed by Kinexus Bioinformatics). Duplicate signals were averaged. The ratio of fluorescent signal of dye 2:dye 1 (LTED:parental) was then calculated, and antibodies which yielded a mean change of ≥1.4-fold were noted. We then compared the lists of antibodies across all 4 pairs of LTED/parental cell lines, and generated the list of commonly altered proteins shown in Figure 1D.

Immunoblotting. Cells were lysed in 1% NP-40 buffer plus protease and phosphatase inhibitors, sonicated for 10 sec., and centrifuged at 14*k* rpm for 10 min as described in ref. (1). Protein was quantitated using BCA assay (Pierce). Lysates were subjected to SDS-PAGE and transferred to nitrocellulose. Primary antibodies for immunoblotting included P-IGF-IRβ_{Y1131}/P-InsRβ_{Y1146}, P-AKT$_{S473}$, P-AKT$_{T308}$, P-EGFR$_{Y1173}$, P-HER2$_{Y1248}$, P-HER3$_{Y1289}$, (Cell Signaling), IGF-IRβ, InsRβ, HER3 (Santa Cruz), and Actin (Sigma). Blots were washed, then probed with HRP-tagged secondary antibodies (sheep-anti-mouse Ig and donkey-anti-rabbit Ig, Amersham). Blots were again washed, and signal was detected using ECL substrate (Amersham) or Supersignal ELISA Pico CL substrate (Pierce).

siRNA transfection. Cells were transfected in 100-mm dishes with siRNA using HiPerfect transfection reagent as per manufacturer's protocol (Qiagen). siRNAs targeting *IGF-IR* (cat. # Hs_IGF1R_1), *InsR* (cat. # Hs_INSR_2), or non-silencing control (cat. # 1027281) were obtained from Qiagen. The next day, cells were reseeded in 12-well plates (MCF-7 lines at 2.5x10^4/well; other lines at 4x10^4/well) for cell proliferation assays, or in 6-well plates for immunoblotting, all in 10% DCC-FBS. In cell proliferation assays, medium was replenished the next day, and again three days later. Cells were trypsinized and counted at 6 days post-transfection using a Coulter counter. For immunoblotting assays, protein lysates were collected at three days post-transfection.

Anchorage-independent colony formation assay. Cells were seeded at $3x10^4$/well in 6-well plates in 0.4% low-melting-point agarose in 5% DCC-FBS. Cells were treated in triplicate ± 200 nM BEZ235, 1 μM AEW541, 20 nM RAD001, or 1 μM lapatinib ditosylate. Eight to 17 days later, plates were scanned and colonies 25-250 μm in diameter were counted using GelCount software (Oxford Optronix). Wells were visually inspected to confirm drug effects. Treatments were compared within each cell line by ANOVA followed by Bonferroni post-hoc test. LTED cells were compared to parental controls by *t*-test. $*p<0.05$ was considered significant.

Crystal Violet Staining assay. Cells were seeded in 6-well plates ($2.5x10^4$/well). Cells were treated with 10% DCC-FBS ± 200 nM BEZ235 (2), 1 μM AEW541 (3), 20 nM RAD001 [(4), all provided by Novartis], or 1 μM lapatinib ditosylate (GW-572016, LC Laboratories). Media and inhibitors were replenished every 2-3 days until 40-60% confluency was achieved in control wells. Cells were then fixed and stained with 20% methanol/80% water/0.5% crystal violet for 20 min., washed with water, and dried. Crystal violet staining intensity was quantified by scanning plates using an Odyssey Infrared Imaging System (LI-COR Biosciences), followed by analysis using manufacturer's software.

Apoptosis assay. Cells were seeded in triplicate in 100-mm dishes (10^6 cells/dish), and treated with 1% DCC-FBS ± 200 nM BEZ235 or 20 nM RAD001 for three days. Cells were fixed, processed as per ApoBrdU kit manufacturer's protocol (Phoenix Flow Systems), and analyzed by flow cytometry (10,000 events). Propidium iodide-stained sub-G1 and FITC-positive apoptotic cells were gated and quantitated.

Gene expression microarray analysis of cell lines. Cells were seeded in 100-mm dishes in triplicate. The following day, medium was changed to IMEM + 10% DCC-FBS. RNA was harvested 24 hours later from subconfluent cells using Trizol (Invitrogen), followed by RNeasy column clean-up and DNase digestion (Qiagen). Bioanalyzer microfluidic assay (Agilent) was used to assess RNA integrity. Spectrophotometric and fluorometric methods were combined to quantitate protein and nucleic acids present in the sample, and to ensure quality control. RNA was prepared for microarray analysis using the GeneChip One-Cycle Target

Labeling and Control Reagents kit (Affymetrix). Biotinylated cRNA (15 µg) was fragmented and hybridized to an Affymetrix GeneChip HG_U133_Plus_2.0 Array (performed in triplicate). Hybridized cRNA was detected using streptavidin coupled to phycoerythrin. GeneChips were scanned using GeneChip Scanner 3000 7G Plus 2 and GeneChip Operating System (GCOS, Affymetrix). Default values were used to grid images (.DAT) and generate .CEL and .CHP files. Data files are available on the Gene Expression Omnibus (GSE19639).

Microarray data were analyzed using R software (www.r-project.org). The Robust Multiarray Average (RMA) method was applied to the pre-processing procedure for the $\log_2$-transformed gene expression levels. Genes included for further analysis were selected based on False Discovery Rate (FDR)-adjusted *p*-value using *t*-tests, as well as the fold change method (5) where parental $\log_2$ gene expression values (mean of triplicates) were subtracted from LTED values ($LTED_{mean}$ - $parental_{mean}$). The moderated *t*-statistic was generated using empirical Bayes shrinkage method for each gene. The Benjamini-Hochberg multiple testing correction-based FDR method was next applied to calculate the adjusted *p*-value for each gene.

For Ingenuity Pathways Analysis (Ingenuity Systems) to group gene products by biological function, sets of genes with expression altered between each pair of LTED and parental cells ≥ 1.5-fold ($p \leq 0.05$) were used.

For Connectivity Mapping (6), probe sets with expression altered between each pair of LTED and parental cells ≥1.3-fold (FDR-adjusted $p \leq 0.05$) were compared using a Venn diagram to identify those commonly and concordantly dysregulated in all 4 cell lines. This common LTED probe set generated using Affymetrix HG_U133_Plus_2 arrays was filtered (using NetAffx www.affymetrix.com/analysis/index.affx) for compatibility with the Affymetrix HG_U133A array platform that was used to generate the Connectivity Map (the U133A platform has roughly ½ of the probe sets included in the U133_Plus_2 platform). The resulting set of 45 probe sets (covering 35 genes) was then used to query the Connectivity Map.

Reverse phase protein lysate microarray analysis (RPPA).

Protein was extracted from 64 hormone receptor-positive primary human breast tumors, and RPPA was performed as described previously in refs. (7-18). Patients were treated with adjuvant aromatase inhibitor therapy (34 received anastrozole, 3 received letrozole), tamoxifen therapy (*n*=23), an unknown endocrine therapy (*n*=1), or no endocrine therapy (*n*=3). Briefly, lysis buffer was used to lyse frozen tumors by homogenization. Tumor lysates were normalized to 1 µg/µL concentration using BCA assay, boiled with 1%

SDS, and the supernatants were manually diluted in six or eight 2-fold serial dilutions with lysis buffer. An Aushon Biosystems (Burlington, MA) 2470 arrayer created 1,056-sample arrays on nitrocellulose-coated FAST slides (Schleicher & Schuell BioScience, Inc.) from the serial dilutions. Slides were then probed with validated primary antibodies against P-AKT$_{S473}$ (Cell Signaling, cat. # 9271), AKT (Cell Signaling, cat. # 9272), P-S6$_{S240/244}$ (Cell Signaling, cat. # 2215), P-GSK3$\alpha/\beta_{S21/9}$ (Cell Signaling, cat. # 9331), GSK3α/β (Santa Cruz, cat. # SC-7291), EGFR (Santa Cruz, cat. # SC-03), ER (Lab Vision, cat. # Sp1), Src (Upstate Biotechnology, cat. # 05-184), P-PKCα_{S657} (Upstate Biotechnology, cat. # 06-822), P-IGF-IR$\beta_{Y1135/1136}$ (Cell Signaling, cat. # 3024; crossreacts with P-InsRβ_{Y1131}), and IGF-IRβ (Cell Signaling, cat # 3027). The antibody signal was next amplified using a DakoCytomation–catalyzed system. A secondary antibody was used as a starting point for amplification. The slides were scanned, analyzed, and quantitated using Microvigene software (VigeneTech Inc.) to generate serial dilution–signal intensity curves for each sample with the logistic fit model: $\ln(y) = a + (b - a) / (1 + \exp\{c^*[d - \ln(x)]\})$. A representative natural logarithmic value of each sample curve on the slide (curve average) was then used as a relative quantification of the amount of each antigen in each sample. These amounts were expressed as a $\log_2$-mean centered value after correction for protein loading using the average expression levels of over 50 proteins as previously described.

P-AKT$_{S473}$, AKT, P-S6$_{S240/244}$, P-GSK3$\alpha/\beta_{S21/9}$, GSK3α/β, EGFR, ER, Src, and P-PKCα_{S657} data were hierarchically clustered across the *tumors* and *antigens* axes using XCluster software (19); heatmaps were generated using Treeview software (20). Kaplan-Meier recurrence curves generated for each tumor/patient cluster were compared using log-rank testing. Cox PH univariate regression was used to assess the association of PI3K cluster effect with recurrence-free survival. To avoid overfitting, multivariate analyses were performed using PI3K cluster effect with each of the following covariates individually: clinical stage (TNM staging), type of endocrine therapy, use of adjuvant chemotherapy, age, nuclear grade.

In order to assess the relationship between the degree of IGF-IR activation in primary tumors and recurrence-free survival, we first calculated the ratio of P-IGF-IRβ to IGF-IRβ for each tumor. Cox Proportional Hazards (PH) regression was used to assess the association of P-IGF-IRβ/IGF-IRβ ratio with recurrence. Patients were then dichotomized based on the mean cutoff of P-IGF-IRβ/IGF-IRβ ratio, and Kaplan-Meier recurrence curves for patients with high vs. low P-IGF-IRβ/IGF-IRβ ratio were compared by the log-rank test.

References for Supplemental Methods

1. Miller, T.W., et al. 2009. Loss of Phosphatase and Tensin homologue deleted on chromosome 10 engages ErbB3 and insulin-like growth factor-I receptor signaling to promote antiestrogen resistance in breast cancer. *Cancer Res* 69:4192-4201.
2. Maira, S.M., et al. 2008. Identification and characterization of NVP-BEZ235, a new orally available dual phosphatidylinositol 3-kinase/mammalian target of rapamycin inhibitor with potent in vivo antitumor activity. *Mol Cancer Ther*.
3. Garcia-Echeverria, C., et al. 2004. In vivo antitumor activity of NVP-AEW541-A novel, potent, and selective inhibitor of the IGF-IR kinase. *Cancer Cell* 5:231-239.
4. Schuler, W., et al. 1997. SDZ RAD, a new rapamycin derivative: pharmacological properties in vitro and in vivo. *Transplantation* 64:36-42.
5. Guix, M., et al. 2008. Acquired resistance to EGFR tyrosine kinase inhibitors in cancer cells is mediated by loss of IGF-binding proteins. *J Clin Invest* 118:2609-2619.
6. Lamb, J., et al. 2006. The Connectivity Map: using gene-expression signatures to connect small molecules, genes, and disease. *Science* 313:1929-1935.
7. Charboneau, L., et al. 2002. Utility of reverse phase protein arrays: applications to signalling pathways and human body arrays. *Brief Funct Genomic Proteomic* 1:305-315.
8. Cheng, K.W., Lu, Y., and Mills, G.B. 2005. Assay of Rab25 function in ovarian and breast cancers. *Methods Enzymol* 403:202-215.
9. Hennessy, B.T., et al. 2009. Characterization of a naturally occurring breast cancer subset enriched in epithelial-to-mesenchymal transition and stem cell characteristics. *Cancer Res* 69:4116-4124.
10. Hennessy, B.T., et al. 2007. Pharmacodynamic markers of perifosine efficacy. *Clin Cancer Res* 13:7421-7431.
11. Hu, J., et al. 2007. Non-parametric quantification of protein lysate arrays. *Bioinformatics* 23:1986-1994.
12. Iwamaru, A., et al. 2007. Silencing mammalian target of rapamycin signaling by small interfering RNA enhances rapamycin-induced autophagy in malignant glioma cells. *Oncogene* 26:1840-1851.
13. Murph, M.M., et al. 2008. Individualized molecular medicine: linking functional proteomics to select therapeutics targeting the PI3K pathway for specific patients. *Adv Exp Med Biol* 622:183-195.
14. Sheehan, K.M., et al. 2005. Use of reverse phase protein microarrays and reference standard development for molecular network analysis of metastatic ovarian carcinoma. *Mol Cell Proteomics* 4:346-355.
15. Stemke-Hale, K., et al. 2008. An integrative genomic and proteomic analysis of PIK3CA, PTEN, and AKT mutations in breast cancer. *Cancer Res* 68:6084-6091.
16. Tibes, R., et al. 2006. Reverse phase protein array: validation of a novel proteomic technology and utility for analysis of primary leukemia specimens and hematopoietic stem cells. *Mol Cancer Ther* 5:2512-2521.
17. Vasudevan, K.M., et al. 2009. AKT-independent signaling downstream of oncogenic PIK3CA mutations in human cancer. *Cancer Cell* 16:21-32.
18. Wulfkuhle, J.D., Edmiston, K.H., Liotta, L.A., and Petricoin, E.F., 3rd. 2006. Technology insight: pharmacoproteomics for cancer--promises of patient-tailored medicine using protein microarrays. *Nat Clin Pract Oncol* 3:256-268.
19. Shenkin, P.S., McDonald, D.Q. 1994. Cluster Analysis of Molecular Conformations. *J. Comput. Chem.* 15:899-916.
20. Eisen, M.B., Spellman, P.T., Brown, P.O., and Botstein, D. 1998. Cluster analysis and display of genome-wide expression patterns. *Proc Natl Acad Sci U S A* 95:14863-14868.